*Journal of Ceramic Processing Research. Vol. 25, No. 5, pp. 814~826 (2024)*
*(Received 26 June 2024, Received in revised form 4 August 2024, Accepted 5 September 2024)*
*https://doi.org/10.36410/jcpr.2024.25.5.814*

J O U R N A L O F
**Ceramic Processing Research**

# Investigation of mechanical properties of mullite-calcium oxide-zirconium dioxide ceramics

**Mehmet Akif Hafızoğlu[a,*], Ahmet Akkuş[b] and Ömer Karabey[c]**
[a]*Dicle University, Department of Mechanical Engineering, Diyarbakır, Turkey*
[b]*Sivas Cumhuriyet University, Department of Mechanical Engineering, Sivas, Turkey*
[c]*Bitlis Eren University, Department of Mechanical Engineering, Bitlis, Turkey*

**In this study, Calcium Oxide (CaO) - Zirconium Dioxide ($ZrO_2$) ceramics and their mullite-doped composite ceramics, which are among the advanced technology ceramics, are examined. During the production phase of the samples, first monoclinic zirconium dioxide was stabilized with calcium oxide (calcia) to obtain stabilized $ZrO_2$. Subsequently, mullite additive was added to these composite mixtures at rates ranging from 0% to 10% by weight, and samples were produced. Not only the effect of mullite additive but also sintering temperature and durations on the microstructure and mechanical properties of CaO-$ZrO_2$ ceramics was investigated. For each sample, sintering temperature parameters were determined to be in the range of 1500 ºC-1600 ºC, and sintering time parameters were determined to be in the range of 1-5 hours. The test and microstructural analysis results demonstrate that the introduction of mullite into the CaO-stabilized $ZrO_2$ composites significantly enhanced the wear resistance. Moreover, it is discerned that sintering at comparatively lower temperatures and for shorter durations provides an augmentation in three-point bending strength, albeit accompanied by a general decrease in hardness.**

**Keywords: Calcium oxide, Zirconium dioxide, Mullite, Mechanical properties, Wear.**

## Introduction

Zirconium dioxide and its various composites, which are in the group of advanced technological ceramics, are very popular for many technological and scientific studies. Due to their good mechanical properties, notable corrosion resistance, low thermal conductivities, robust stability under high temperatures, and chemical stabilities, the composites exhibit notable attributes [1-3]. These materials are highly favored for a myriad of applications, serving as pivotal components in refractory materials, high-temperature industrial furnaces, components resistant to wear, and diverse cutting tools, among a plethora of other fields. In particular, Calcium oxide-zirconium dioxide composites are biocompatible and can be used in biomedical implants and prosthetics and can also be used in structural applications where high mechanical strength is required. Their stability, resistance to corrosion and wear make them suitable for dental prosthetics, bone substitutes, other medical applications and structural applications [3-6].

The high-purity form of zirconia ($ZrO_2$) manifests three distinct polymorphs contingent upon temperature variations: the monoclinic phase retains stability up to temperatures of 1170 ºC, beyond which, the mutation to the tetragonal phase commences, maintaining stability up to temperatures reaching 2370 ºC [1]. Subsequently, from this threshold to the melting temperature at 2680 ºC, the cubic zirconia phase emerges [1]. With cooling, conversion from the tetragonal crystalline phase to the monoclinic crystalline phase begin again. The conversion to the monoclinic phase is very important because this conversion causes volumetric changes of around 3-5%, causing cracks [1, 3].

In order to mitigate such transformations and stabilize zirconia, incorporation of stabilizers or additives that help stabilizing and toughening has become commonplace. The introduction of stabilizers serves to lower the temperature thresholds for transformations, curtail volumetric expansion or contraction, and impede polymorphic transitions [2, 3]. Various stabilizers or additives that help stabilizing and toughening, including alumina [4, 5], calcia [6], ceria [7, 8], magnesia [9], silica [10, 11], titania [12, 13], and yttria [14-17], either individually or in combination, serve to stabilize zirconia in either the tetragonal (t-$ZrO_2$) or cubic (c-$ZrO_2$) forms at lower temperatures. Through the incorporation of stabilizers, the attainment of partially or fully stabilized zirconia is possible. Thereby enabling the realization of advanced mechanical properties, including heightened hardness, bending strength, and fracture toughness [1, 3, 16, 18].

In this study, calcia was used to stabilize zirconia.

*Corresponding author:
Tel : +90 412 241 10 00 / 3517
Fax: +90 412 248 82 18
E-mail: makif.hafizoglu@dicle.edu.tr

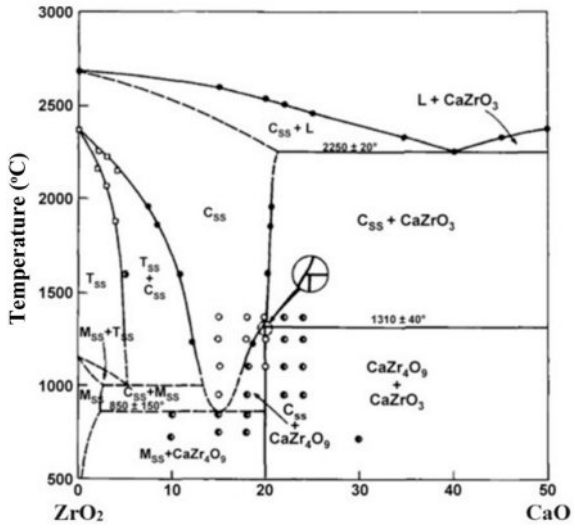


**Fig. 1.** $ZrO_2$-CaO binary phase diagram (mol %) [19].

The composition was formed as 10 mol% CaO-90 mol% $ZrO_2$. The CaO-$ZrO_2$ binary phase diagram is shown in Fig. 1. According to the phase diagram, the tetragonal ($T_{ss}$) + cubic ($C_{ss}$) phase region was studied depending on the sintering temperatures and times with 10 mol% CaO.

Zirconia notably surpasses other ceramics in terms of mechanical prowess, yet akin to its counterparts, it remains brittle and resistant to deformation at ambient temperatures. Consequently, efforts to enhance the toughness of zirconia-based materials are imperative. To bolster toughness, transformation toughening, reinforcement with nanofibers or nanotubes, and other mechanisms for energy absorption are employed within ceramic composite matrices [17, 18]. The reinforcement technique involves the incorporation of ceramic whiskers, fibers, or particles into the primary phase, thereby augmenting both strength and toughness by creating a physical impediment to crack propagation. Whiskers, possessing superior tensile strength compared to polycrystalline materials, serve as effective barriers against crack propagation, thereby bolstering the fracture toughness of zirconia [17, 18].

Characterized by its perfect stability in the $Al_2O_3$-$SiO_2$ binary system, affordable price and superior refractory properties, whisker structured mullite has garnered significant attraction in technological applications [17, 20-23]. Its attributes, including low coefficient of thermal expansion, elevated melting point, resistance to creep, chemical stability, and satisfactory hardness, render it an unparalleled candidate for enhancing the fracture toughness of zirconia through reinforcement as a secondary phase, thereby improving various mechanical properties [17, 22]. Consequently, incorporating mullite into the zirconia structure emerges as a promising and strong alternative [17].

In addition to stabilizing and toughening studies, the sintering temperature and duration play a crucial role and necessitate meticulous scrutiny as they influence the characteristics of ceramics by modifying both the microstructure and crystalline phases. Researches concentrate on investigating how variations in sintering temperatures and durations impact the microstructural composition and mechanical properties of mullite-calcia-zirconia ceramics. One of the important mechanical properties affected by sintering temperature and duration is resistance to wear. Some of the most common wear testing methodologies generally used for this purpose are: block on ring, pin on disc, ball on disc, reciprocating sliding wear test methods. Each test method has its own strengths and weaknesses. The main factors used as parameters are wear load, wear rate (such as setting the number of revolutions on the device), applied time, wear environment (dry wear, oily environment, water or different wear environments using various chemicals). When choosing the appropriate wear test methodology and determining the wear parameters, the most appropriate method and parameters are selected by considering the conditions that the ceramic composite may encounter according to its place of use and purpose.

Numerous inquiries have delved into the wear properties of ceramic composite materials and the influence of mullite on mechanical attributes. For instance, Boyraz and Akkuş [20] explored the wear properties of specimens derived from sintering composite mixtures of mullite, aluminum titanate, and porcelain powders in varied compositions and ratios at diverse temperatures and durations using the block-on-ring wear method and with dry sliding conditions. Their findings underscored the efficacy of mullite in boosting the wear resistance of ceramics. Likewise, Huang et al. [24] elucidated the significant impact of porosity, hardness, density, and bending strength on the wear characteristics in oily environment and by the pin-on-disc wear method for samples incorporating mullite into zirconia. Notably, the 4 mol% mullite added sample showcased superior wear resistance and bending strength compared to its counterparts, underscoring the nuanced interplay of mechanical characteristics.

In this study, ceramic composite samples were fabricated by sintering a blend of CaO-$ZrO_2$ powders at various temperatures and durations. Furthermore, ceramic composite samples augmented with 5% and 10% mullite additive by weight were produced by incorporating mullite into the CaO-$ZrO_2$ powder mixture, employing the same sintering parameters. The resultant samples underwent a series of physical, mechanical, and characterization tests to examine the impacts of sintering temperatures and durations and the addition of mullite reinforcement on their physical, microstructural, and mechanical properties.

## Materials and Experimental Details

Raw materials, including silica and alumina powders

from Eczacıbası Holding Company, calcia powder from Alfa Aesar, and zirconia from Handan Yaxiang Chemicals Trading Co, were procured. The powder mixtures were mixed in acetone environment using mechanical alloying method. Subsequently, upon completion of the mixing process, they underwent drying in an oven at temperatures ranging from 100 ºC to 110 ºC for a duration of 24 hours. Mullite synthesis involves preparing a silica-alumina mixture with stoichiometric ratios, which is then fired in air at 1600 ºC for 3 hours. The calcia-zirconia composite underwent firing at 1300 ºC for 2 hours to induce composite phase formation, followed by grinding and sieving processes. Using powder metallurgy technique, zirconia ceramic composites without mullite (0%), with 5%, and 10% mullite content by weight were prepared.

The samples were designated with codes representing their characteristics: for example, 15503CaZ0M, 15503CaZ5M, and 15503CaZ10M. These codes mean as follows: "15503" indicating a sintering temperature of 1550 ºC and a sintering time of 3 hours; "CaZ" representing calcium oxide stabilized zirconia; and suffixes denoting the mullite content, with "0M" indicating mullite-free (0% by weight), "5M" signifying 5% by weight mullite and "10M" representing a 10% by weight addition of mullite. The coding of all other samples is done with the same logic.

After grinding and drying, the composite powders underwent compression using a uniaxial press machine under a load of 200 MPa. Sintering of green compacts occurred in air conditions with heating rates of 5 ºC $min^{-1}$ for varying durations (1 hour, 3 hours, and 5 hours) at temperatures of 1500 ºC, 1550 ºC, and 1600 ºC in a high-temperature furnace. 27 different samples were produced using 3 different mullite mixture amounts, 3 different sintering temperatures, and 3 different sintering time parameters. The production process of the composites typically involves five sequential steps, shown in Fig. 2.

Subsequently, microstructure examinations, phase analyses, and evaluations of mechanical (wear, 3-point bending strength, hardness) and physical properties (% shrinkage, porosity, water absorption, density) were conducted on the mullite-added calcia stabilized zirconia ceramic composites.

For three-point bending strength testing, a Shimadzu-brand tensile-compression equipment was utilized. The speed of the crosshead was 0.5 $mm.min^{-1}$. The bending strength was ascertained by computing the mean of 5 measurements for each sample, employing the formula (1):

$$\sigma = \frac{3}{2} PL/(bh^2) \quad (1)$$

Where P represents the maximum force, L denotes the distance between supports, h signifies the height of samples, and b stands for the width of samples.

Following the initial process steps, which include sanding with sandpapers ranging from 180 to 2500 grit (180, 320, 600, 1200, and 2500) respectively, each sample underwent a polishing procedure. Hardness evaluations were performed utilizing a micro-Vickers hardness measuring device manufactured by Mitutoyo, with a 1 kg load applied for a period of 10 seconds.

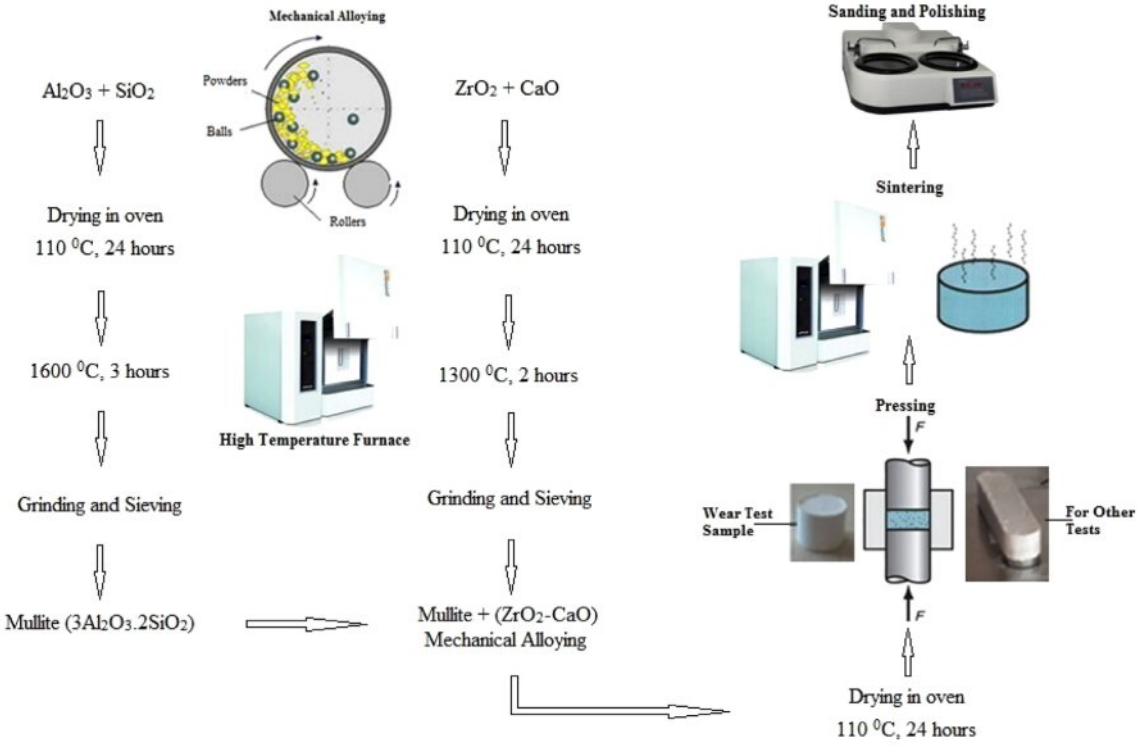


**Fig. 2.** Production stages diagram of composites.

The bending strength calculations were derived from the mean of 5 measurements for each sample.

For wear tests of samples, Plint wear tester was used. Steel disc was used for tests. The tests were conducted at 400 rpm for each sample, with forces ranging from 50 N to 150 N (50, 100, 150) applied and durations of five, ten, and fifteen minutes allocated for wear testing. Precise weighing scales were utilized to measure wear rates before and after testing.

XRD analysis, utilizing CuKα radiation, was employed to ascertain the phases present within the samples (Bruker AXS D8 Advance brand; $\theta=10^0$-$90^0$, $0.002^0$, 6 mA-80 mA, 20 kV-60 kV). The Panalytical X'Pert program facilitated phase determination based on microstructural data.

The microstructural characterization studies were done with TESCAN Mira3XMU FE-SEM brand scanning electron microscope and using energy dispersion spectrum.

The findings are presented through graphics and tables, followed by comprehensive evaluations based on the outcomes.

## Results and Discussions

In this section, physical test results, mechanical test results, scanning electron microscope, and XRD analyzes are given. The tables present comprehensive details of the physical and mechanical test results for each specimen.

Tables 1, 2, 3 furnish physical measurements such as bulk density, relative density, water absorption, porosity, and shrinkage values. The density values depicted in Fig. 3 are crucial as they offer insight into other physical measurements.

Based on the findings for the samples lacking mullite (CaZ0M), the values of experimental or bulk density, relative density, and shrinkage are higher than the mullite-added samples. Because mullite has low density and steadfast stability. With escalating sintering temperature and duration, a discernible trend emerges whereby shrinkage values escalate, while water absorption and porosity register a concurrent decline in mullite-free samples. Therefore, values of bulk and relative density increase in these samples.

While the shrinkage, bulk, and relative density measurements of 5% (CaZ5M) and 10% (CaZ10M) mullite-added samples are highest for 1500 and 1550 coded samples sintered for 3 hours; For samples with code 1600, these values are highest in samples sintered for 1 hour. At extremely high sintering temperatures

**Table 1.** Physical test results for CaZ0M samples.

| Samples | Bulk density ($g/cm^3$) | Relative density (%) | Water absorption (%) | Porosity (%) | Shrinkage (%) |
|---|---|---|---|---|---|
| 15001CaZ0M | 4.773 | 86.768 | 3.412 | 13.230 | 9.792 |
| 15003CaZ0M | 5.007 | 91.081 | 2.381 | 8.919 | 11.524 |
| 15005CaZ0M | 5.162 | 93.891 | 1.755 | 6.109 | 12.202 |
| 15501CaZ0M | 5.085 | 92.495 | 1.844 | 7.505 | 11.624 |
| 15503CaZ0M | 5.255 | 95.579 | 1.033 | 4.421 | 12.458 |
| 15505CaZ0M | 5.321 | 96.791 | 0.788 | 3.209 | 12.857 |
| 16001CaZ0M | 5.166 | 94.040 | 1.204 | 5.960 | 12.430 |
| 16003CaZ0M | 5.230 | 95.130 | 0.415 | 4.871 | 12.545 |
| 16005CaZ0M | 5.260 | 95.673 | 0.360 | 4.327 | 12.762 |

**Table 2.** Physical test results for CaZ5M samples.

| Samples | Bulk density ($g/cm^3$) | Relative density (%) | Water absorption (%) | Porosity (%) | Shrinkage (%) |
|---|---|---|---|---|---|
| 15001CaZ5M | 5.042 | 94.398 | 0.407 | 5.602 | 11.190 |
| 15003CaZ5M | 5.078 | 95.076 | 0.390 | 4.924 | 11.399 |
| 15005CaZ5M | 5.067 | 94.874 | 0.401 | 5.126 | 11.268 |
| 15501CaZ5M | 5.074 | 95.001 | 0.728 | 4.999 | 11.369 |
| 15503CaZ5M | 5.103 | 95.537 | 0.591 | 4.463 | 11.360 |
| 15505CaZ5M | 5.051 | 94.574 | 0.690 | 5.426 | 11.155 |
| 16001CaZ5M | 5.102 | 95.527 | 0.596 | 4.473 | 11.381 |
| 16003CaZ5M | 5.062 | 94.774 | 0.806 | 5.226 | 11.071 |
| 16005CaZ5M | 5.043 | 94.417 | 0.828 | 5.583 | 10.920 |

**Table 3.** Physical test findings for CaZ10M samples.

| Samples | Bulk density ($g/cm^3$) | Relative density (%) | Water absorption (%) | Porosity (%) | Shrinkage (%) |
|---|---|---|---|---|---|
| 15001CaZ10M | 4.715 | 90.798 | 1.133 | 9.202 | 9.761 |
| 15003CaZ10M | 4.741 | 91.299 | 1.011 | 8.701 | 9.813 |
| 15005CaZ10M | 4.701 | 90.528 | 1.202 | 9.472 | 9.521 |
| 15501CaZ10M | 4.718 | 90.848 | 0.885 | 9.152 | 9.251 |
| 15503CaZ10M | 4.751 | 91.497 | 0.829 | 8.503 | 9.438 |
| 15505CaZ10M | 4.664 | 89.808 | 0.964 | 10.192 | 9.083 |
| 16001CaZ10M | 4.709 | 90.685 | 0.854 | 9.315 | 9.387 |
| 16003CaZ10M | 4.629 | 89.142 | 1.253 | 10.858 | 8.885 |
| 16005CaZ10M | 4.558 | 87.774 | 1.338 | 12.226 | 8.633 |

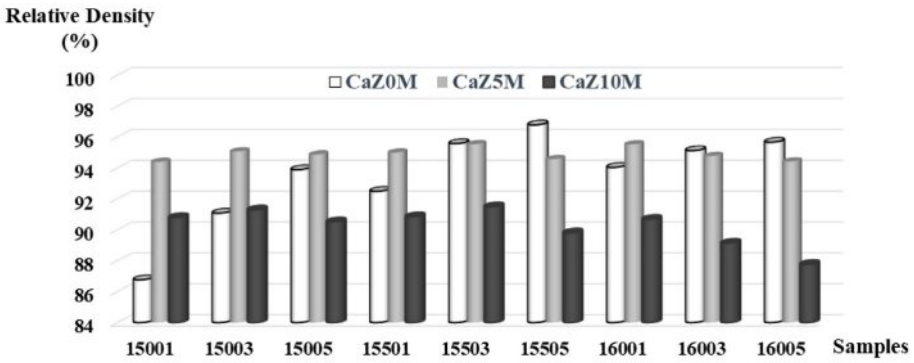


**Fig. 3.** Relative density results graph for all samples.

and times, a decline in shrinkage, bulk, and relative density values ensues due to microstructural anomalies such as excessive grain growth, heightened porosity, and potential phase changes.

It is understood that the highest shrinkage, bulk, and relative density rates for all samples among both mullite-inclusive and mullite-absent belong to samples coded 1550. This result shows that the optimum sintering temperature for shrinkage, bulk, and relative density values for these composite samples is 1550. And for optimum sintering duration, it can be concluded that 5 hours for mullite-free samples and 3 hours for mullite-added samples are optimum.

The effects of mullite additive ratio and sintering temperature and time on the hardness and three-point bending strength properties of CaZ0M, CaZ5M, and CaZ10M samples were investigated. Table 4, 5, and 6 show these findings.

**Table 4.** Micro hardness - bending strength tests results for CaZ0M samples.

| Samples | Hardness (HV) | 3-Point Bending Strength (MPa) |
|---|---|---|
| 15001CaZ0M | 489.98 | 69.89 |
| 15003CaZ0M | 689.03 | 67.13 |
| 15005CaZ0M | 702.25 | 63.52 |
| 15501CaZ0M | 640.38 | 85.01 |
| 15503CaZ0M | 801.92 | 81.43 |
| 15505CaZ0M | 905.18 | 65.32 |
| 16001CaZ0M | 705.40 | 62.01 |
| 16003CaZ0M | 953.87 | 60.85 |
| 16005CaZ0M | 977.84 | 25.29 |

**Table 5.** Micro hardness - bending strength tests results for CaZ5M samples.

| Samples | Hardness (HV) | 3-Point Bending Strength (MPa) |
|---|---|---|
| 15001CaZ5M | 644.20 | 169.79 |
| 15003CaZ5M | 690.65 | 138.64 |
| 15005CaZ5M | 623.80 | 111.36 |
| 15501CaZ5M | 550.75 | 113.92 |
| 15503CaZ5M | 557.62 | 60.59 |
| 15505CaZ5M | 435.43 | 52.39 |
| 16001CaZ5M | 551.63 | 80.80 |
| 16003CaZ5M | 519.03 | 50.96 |
| 16005CaZ5M | 457.65 | 15.66 |

**Table 6.** Micro hardness-bending strength tests results for CaZ10M samples.

| Samples | Hardness (HV) | 3-Point Bending Strength (MPa) |
|---|---|---|
| 15001CaZ10M | 427.33 | 134.14 |
| 15003CaZ10M | 458.95 | 105.42 |
| 15005CaZ10M | 448.78 | 91.21 |
| 15501CaZ10M | 415.63 | 62.94 |
| 15503CaZ10M | 418.13 | 58.63 |
| 15505CaZ10M | 393.45 | 41.22 |
| 16001CaZ10M | 421.23 | 101.03 |
| 16003CaZ10M | 359.73 | 67.53 |
| 16005CaZ10M | 330.17 | 53.61 |

With escalating sintering temperature and duration, hardness of mullite-free samples increases, as evidenced by the data presented by both the tabulated results and the hardness results graphics. While the highest hardness value is seen in 16005CaZ0M samples, the lowest value is evident in 16005CaZ10M samples. In mullite-added samples, a general decrement in hardness values is discernible for specimens subjected to higher sintering temperatures and durations. The hardness values of samples incorporating mullite additives generally exhibit a downward trend, diminishing further with an augmentation in the quantity of mullite additive as depicted in Fig. 4. The predominant factor contributing to this situation is the existence of huge pores within the structure of mullite-added samples.

In Fig. 5, bending strength values generally decrease at high sintering temperatures and times. While the highest bending strength value is seen in 15001CaZ5M samples, the lowest value is evident in 16005CaZ5M samples. It is understood that the bending strength data for the mullite-added samples are generally higher than the mullite-free samples. This proves that the mullite additive improved the bending strength in these specimens.

Wear tests were carried out at 400 rpm for each sample. Tests were carried out by applying loads of 150 N, 100 N, 50 N and wear times of 5, 10, 15 minutes for each load. Tables 7, 8, and 9 display the obtained data. Scale with $10^{-4}$ g precision were used for weighing. Wear volumes were calculated by measuring the weight of the samples before and after subjecting them to the specified wear loads and times. The wear quantities of the samples are observed to escalate in tandem with the augmentation of wear time and applied load, as understood by the wear results. This underscores the influence of applied wear load, wear duration, hardness, and microstructural attributes on the resultant wear outcomes. The type of wear seen in the samples in general was adhesive. But it was noted that in some samples, cracks were formed on worn surfaces and very small particles broke off and

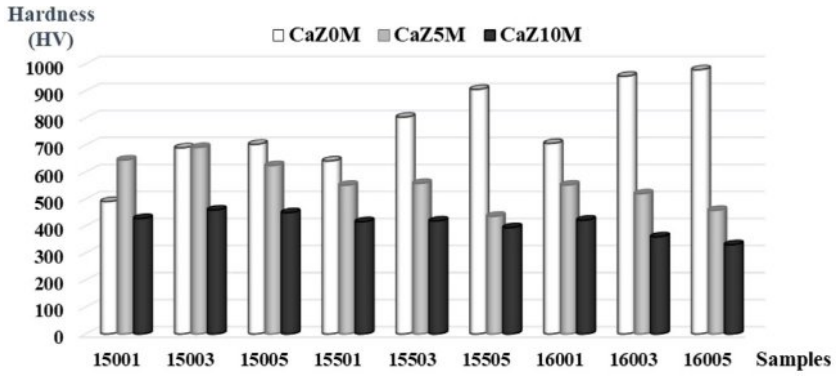


**Fig. 4.** Hardness results graph of samples.

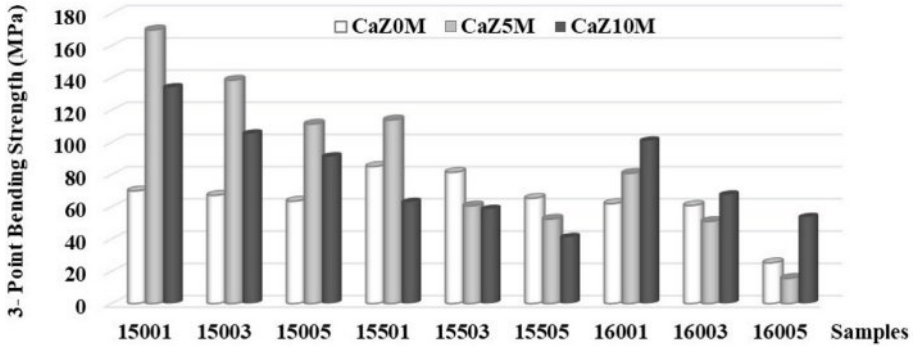


**Fig. 5.** Graph of 3-point bending strength.

**Table 7.** Wear results of CaZ0M samples under various loads and wear durations.

| Samples | 50 N | | | 100 N | | | 150 N | | |
|---|---|---|---|---|---|---|---|---|---|
| | Wear Duration (min.), Wear Volume ($mm^3$) | | | | | | | | |
| | 5 | 10 | 15 | 5 | 10 | 15 | 5 | 10 | 15 |
| 15001CaZ0M | 0.578 | 1.901 | 3.469 | 0.658 | 2.224 | 3.978 | 1.523 | 4.252 | 6.775 |
| 15003CaZ0M | 0.569 | 2.081 | 3.373 | 0.595 | 2.207 | 3.532 | 1.464 | 3.743 | 5.515 |
| 15005CaZ0M | 0.598 | 2.160 | 3.129 | 0.616 | 2.232 | 3.421 | 1.419 | 3.532 | 5.121 |
| 15501CaZ0M | 0.541 | 1.573 | 2.803 | 0.558 | 1.644 | 2.981 | 0.904 | 1.847 | 3.524 |
| 15503CaZ0M | 0.465 | 1.485 | 2.716 | 0.502 | 1.617 | 2.906 | 0.865 | 1.718 | 3.338 |
| 15505CaZ0M | 0.430 | 1.142 | 2.571 | 0.357 | 1.231 | 2.603 | 0.573 | 1.462 | 2.891 |
| 16001CaZ0M | 0.530 | 2.112 | 2.983 | 0.605 | 2.199 | 3.298 | 1.202 | 2.927 | 4.908 |
| 16003CaZ0M | 0.869 | 2.281 | 3.737 | 0.861 | 2.553 | 4.380 | 1.964 | 4.509 | 9.434 |
| 16005CaZ0M | 1.382 | 2.440 | 6.833 | 1.855 | 4.114 | 9.443 | 3.352 | 7.114 | 17.227 |

**Table 8.** Wear results of CaZ5M samples under various loads and wear durations.

| Samples | 50 N | | | 100 N | | | 150 N | | |
|---|---|---|---|---|---|---|---|---|---|
| | Wear Duration (min.), Wear Volume ($mm^3$) | | | | | | | | |
| | 5 | 10 | 15 | 5 | 10 | 15 | 5 | 10 | 15 |
| 15001CaZ5M | 0.040 | 0.179 | 0.298 | 0.159 | 0.238 | 0.337 | 0.161 | 0.399 | 0.537 |
| 15003CaZ5M | 0.847 | 1.260 | 1.516 | 0.256 | 0.937 | 1.647 | 0.924 | 1.319 | 1.792 |
| 15005CaZ5M | 0.079 | 0.237 | 0.375 | 0.178 | 0.257 | 0.414 | 0.296 | 0.474 | 0.632 |
| 15501CaZ5M | 0.315 | 0.552 | 0.690 | 0.315 | 0.611 | 1.045 | 0.355 | 0.512 | 1.401 |
| 15503CaZ5M | 0.607 | 0.980 | 1.641 | 0.962 | 1.417 | 2.507 | 1.704 | 2.513 | 3.447 |
| 15505CaZ5M | 0.297 | 0.455 | 0.772 | 0.238 | 0.544 | 0.867 | 0.554 | 1.465 | 1.574 |
| 16001CaZ5M | 1.093 | 2.160 | 2.736 | 1.104 | 2.469 | 3.208 | 1.216 | 2.814 | 4.655 |
| 16003CaZ5M | 0.879 | 1.079 | 1.399 | 0.894 | 1.319 | 1.738 | 0.934 | 1.399 | 2.677 |
| 16005CaZ5M | 0.296 | 0.355 | 0.552 | 0.793 | 0.927 | 1.307 | 0.857 | 1.167 | 1.542 |

**Table 9.** Wear results of CaZ10M samples under various loads and wear durations.

| Samples | 50 N | | | 100 N | | | 150 N | | |
|---|---|---|---|---|---|---|---|---|---|
| | Wear Duration (min.), Wear Volume ($mm^3$) | | | | | | | | |
| | 5 | 10 | 15 | 5 | 10 | 15 | 5 | 10 | 15 |
| 15001CaZ10M | 0.586 | 1.247 | 1.632 | 0.814 | 1.566 | 1.799 | 0.907 | 1.691 | 2.226 |
| 15003CaZ10M | 0.660 | 1.278 | 1.848 | 0.753 | 1.620 | 2.085 | 0.966 | 1.780 | 2.475 |
| 15005CaZ10M | 0.835 | 1.789 | 2.728 | 0.936 | 2.189 | 3.281 | 1.294 | 2.347 | 3.862 |
| 15501CaZ10M | 0.658 | 1.319 | 2.364 | 0.759 | 1.642 | 2.565 | 0.848 | 1.929 | 2.860 |
| 15503CaZ10M | 0.740 | 1.432 | 2.474 | 0.810 | 1.766 | 2.603 | 0.887 | 2.077 | 2.959 |
| 15505CaZ10M | 0.973 | 1.714 | 2.866 | 1.020 | 2.249 | 3.377 | 1.256 | 2.355 | 3.662 |
| 16001CaZ10M | 0.618 | 1.205 | 1.919 | 0.784 | 1.495 | 2.037 | 0.818 | 1.520 | 2.160 |
| 16003CaZ10M | 0.756 | 1.633 | 3.126 | 0.964 | 1.929 | 3.743 | 1.199 | 2.289 | 4.394 |
| 16005CaZ10M | 0.975 | 1.888 | 3.313 | 1.198 | 2.407 | 4.277 | 1.325 | 2.469 | 4.872 |

caused abrasive wear with increasing the wear time. Fig. 6 compares the wear volume values of all samples with and without mullite additive under 150 N load and a wear time of 15 minutes. It becomes apparent that the addition of mullite typically enhances the wear resistance, resulting in reduced wear volumes. Considering the general results, it can be deduced that 5% mullite-added (CaZ5M) composites have the best wear resistance properties. The main reason why mullite increases the wear resistance in these composites is that the addition

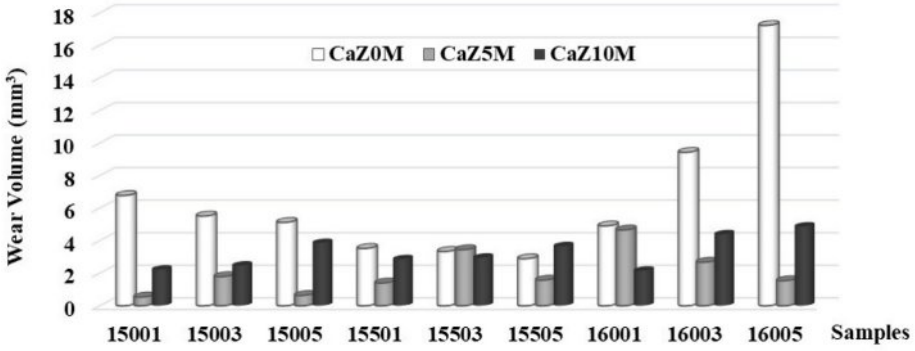


**Fig. 6.** Wear test graph for 150 N load and 15 min duration.

of ceramic whiskers or particles such as mullite to the main phase provides increased strength, bending strength, and toughness. This approach is grounded in the concept of establishing a physical obstruction to hinder crack propagation. Whiskers, possessing greater tensile strength than polycrystalline materials, effectively serve as a barrier to crack advancement [18].

The mullite additive forms a dispersed phase within the zirconia matrix. This phase acts as a physical barrier against the common mechanisms of wear, namely crack initiation and crack propagation, and ensures that the zirconia grains are held together and make it difficult for them to break apart under the influence of wear, thus reducing the effect of damage [24]. Thus, the microstructural reinforcement provided by mullite improves the overall durability of the composite and makes it more resistant to wear.

During the friction and wear test, the samples are exposed to micro scratches and breaks. However, while slight adhesive wear occurred in samples containing mullite, which have higher bending strength and lower brittleness compared to samples without mullite, severe wear was observed in samples without mullite due to brittleness and fragility, with particles breaking off from the surface.

For the mullite-free (CaZ0M) samples, the wear resistance changes in direct proportion with the hardness values in general. As the hardness values increase, the wear resistance also increases. However, although higher hardness values were achieved in 1600 coded samples without mullite additive, the wear resistance decreased. Out of all the samples, the 16005CaZ0M sample has the highest hardness value. However, the highest wear volume value belongs to this sample too. Because with escalating sintering temperature and duration, the cubic zirconia phase increases, giving the sample a brittle structure. For 5% mullite-added (CaZ5M) samples, the wear resistance changes inversely with the hardness values in general. As the hardness values increase, the wear resistance decreases.

In the 10% mullite-added (CaZ10M) samples, with escalating sintering temperature and duration, the wear resistance decreased. The absence of tetragonal zirconia in the structure, large pores and excessive grain coarsening occurring at elevated sintering temperatures and durations resulted in this situation.

X-ray diffraction and SEM analyzes were obtained and evaluated for 16005CaZ0M, 16005CaZ5M, and 16005CaZ10M samples. The phases of samples in the X-ray diffraction pattern were defined.

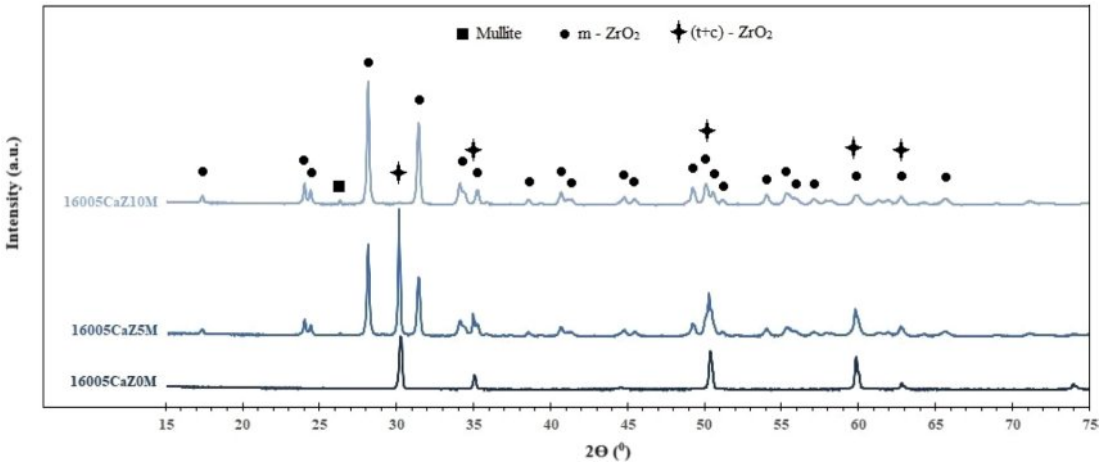


**Fig. 7.** XRD analysis for samples coded as 16005.

Figure 7 exhibits the phases detected in the mullite-free 16005CaZ0M sample, in the mullite-added 16005CaZ5M and 16005CaZ10M samples. These phases are m-$ZrO_2$, t-$ZrO_2$, and c-$ZrO_2$ polymorphs of zirconia and mullite phase.

With escalating sintering temperature and duration, cubic zirconia phase increases significantly. However, while the amount of cubic zirconia phase in the structure increases, tetragonal zirconia phase decreases. The main factors affecting this phase transformation are the sintering temperature and time. As can be understood from the CaO-$ZrO_2$ phase diagram seen in Fig. 1, in the part where the composition ratio is 10 mol% CaO--90 mol% $ZrO_2$, there is a region where the solid cubic phase ($C_{ss}$) and solid tetragonal phase ($T_{ss}$) are seen together in the range of 1500 ºC-1600 ºC. If the temperature increases a little more, the microstructure completely transforms into a solid cubic phase according to the phase diagram at the same composition ratio. As can be understood from here, the cubic phase ratio in the microstructure will also increase as the temperature increases to 1600 ºC. At high sintering temperatures, tetragonal zirconia tends to transform into cubic zirconia due to the decrease in free energy associated with the phase change. Increasing the sintering temperature and time further improves the diffusion and reaction kinetics and supports the stabilization of the cubic phase. Higher temperature facilitates better diffusion and incorporation of CaO stabilizer into the zirconia lattice, resulting in a microstructure with more cubic zirconia. During sintering, zirconia grains grow in size at higher temperatures and times. Larger grains are thermodynamically more favorable in the cubic phase [25]. As a result, the cubic phase increases in structure, while the tetragonal phase naturally decreases.

Nath et al. [26] fabricated partially stabilized zirconia containing 8 mol % calcia and fully stabilized zirconia incorporating 16 mol % calcia. In partially stabilized zirconia samples, the cubic zirconia phase increased at high sintering temperatures that were 1550 ºC and 1585 ºC and they specified that tetragonal zirconia phase decreased significantly. They stated that although the partially stabilized zirconia samples have higher density values than fully stabilized zirconia samples, single-phase cubic zirconia fully stabilized zirconia materials have higher hardness values. Because the tetragonal zirconia and cubic zirconia phases are harder than the monoclinic zirconia phase.

As for the hardness properties, the cubic zirconia phase generally exhibits higher hardness than the tetragonal zirconia phase. The main reason for this is its stable crystal structure and the absence of stress-induced transformation mechanisms. The studies [26-28] demonstrate that fully stabilized cubic zirconia is found to have greater hardness than partially stabilized tetragonal zirconia. The cubic phase is highlighted as having higher hardness but lower toughness compared to the tetragonal phase.

As evidenced by the XRD graph, the structure of the mullite-free 16005CaZ0M sample undergoes a complete transformation into tetragonal zirconia and cubic zirconia phases, attributable to the elevated sintering temperature and duration. Therefore, the hardness values are higher than the other samples. As the mullite additive increased, the amount of monoclinic zirconia in the structure increased significantly and decreased the hardness values.

One of the key mechanisms for enhancing the mechanical properties of zirconia ceramics is the transformation toughening effect associated with the tetragonal phase. When stress is applied, such as during flexural testing, the metastable tetragonal zirconia can transform into the monoclinic phase. This transformation is accompanied by a volume expansion (about 3-5%), which induces compressive stresses around cracks and hinders their propagation. The presence of a higher proportion of tetragonal zirconia leads to more effective transformation toughening, resulting in increased flexural strength [29-31]. The cubic zirconia is more brittle than its tetragonal counterpart. The strength of fully stabilized cubic zirconia can only attain one-half to two-thirds of that of partially stabilized tetragonal zirconia [32]. Therefore, as the amount of cubic zirconia phase in the structure increases, the corresponding decrease in the tetragonal zirconia phase reduces the transformation toughness, which is the transformation from tetragonal zirconia to monoclinic zirconia, and this causes the flexural strength to decrease.

Consistent with the findings of the study [33], our study also demonstrates that an augmentation in the quantities of cubic zirconia and monoclinic zirconia phases leads to a reduction in the amount of tetragonal zirconia phase. Consequently, the conversion from tetragonal zirconia to monoclinic zirconia decreases, resulting in a decrease in both fracture toughness and bending strength. For this reason, the highest bending strength measurements are seen in CaZ5M samples and the lowest bending strength measurements are seen in CaZ10M samples.

Figures 8, 9, and 10 display microstructure images and EDS analyzes of 16005CaZ0M, 16005CaZ5M, and 16005CaZ10M samples. EDS analyzes were made from different areas as general surface scanning (Area 1), point 2, point 3, and point 4. In mullite added samples, mullite is seen in the areas indicated by point 2. As seen in Figs. 9 and 10, mullite transforms into small granular or even fluid shapes and becomes interconnected without a clear form. Mullite is randomly dispersed throughout the zirconia matrix and the zirconia particles in mullite are almost imperceptible. This outcome aligns with the findings reported by Huang et al. [33].

When comparing samples containing mullite with those not containing mullite for flexural strength, not only microstructural defects such as grain growth and large pores but also phase differences occurring in the structure are important. Grain coarsening in samples not

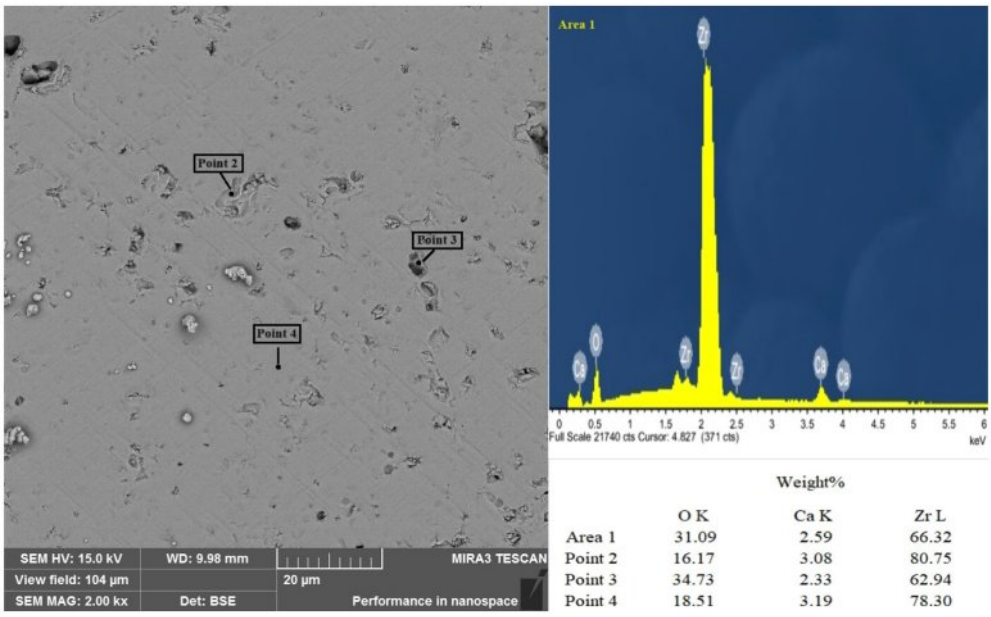


| | Weight% | | |
|---|---|---|---|
| | O K | Ca K | Zr L |
| Area 1 | 31.09 | 2.59 | 66.32 |
| Point 2 | 16.17 | 3.08 | 80.75 |
| Point 3 | 34.73 | 2.33 | 62.94 |
| Point 4 | 18.51 | 3.19 | 78.30 |

**Fig. 8.** Image of SEM - EDS for 16005CaZ0M.

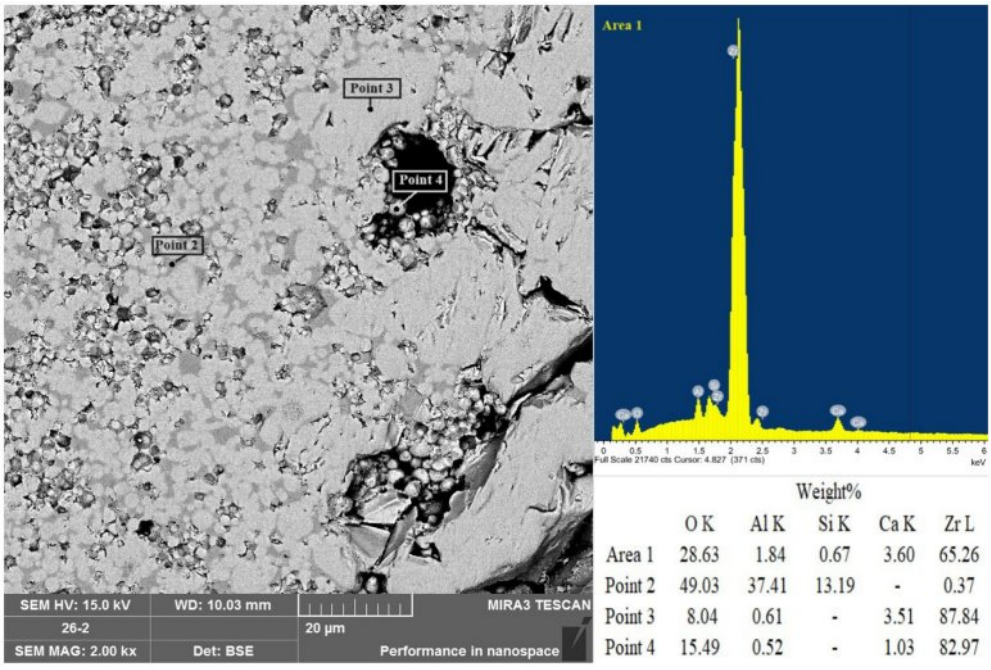


| | Weight% | | | | |
|---|---|---|---|---|---|
| | O K | Al K | Si K | Ca K | Zr L |
| Area 1 | 28.63 | 1.84 | 0.67 | 3.60 | 65.26 |
| Point 2 | 49.03 | 37.41 | 13.19 | - | 0.37 |
| Point 3 | 8.04 | 0.61 | - | 3.51 | 87.84 |
| Point 4 | 15.49 | 0.52 | - | 1.03 | 82.97 |

**Fig. 9.** Image of SEM - EDS for 16005CaZ5M.

containing mullite has an effect that increases the cubic phase as mentioned before [25] and therefore generally decreases the flexural strength. In samples containing mullite, excessive grain growth and microstructural defects such as large pores, which occur with the increase in sintering temperature and time, generally negatively affect the bending strength and reduce these values.

The microstructure images provide insight into the physical characteristics of the samples. Size and amount of the pores increased significantly due to increase in the mullite ratio in the composite mixture. While the hardness values are higher in samples not containing mullite at high sintering temperatures and times; it is observed that the hardness values decrease as the sintering temperature and times increase in samples containing mullite. Therefore, excessive grain growth and large pores negatively affect the hardness of samples containing mullite. In samples not containing mullite, hardness values increased due to the absence of large pores, decreased porosity, increased relative density, and

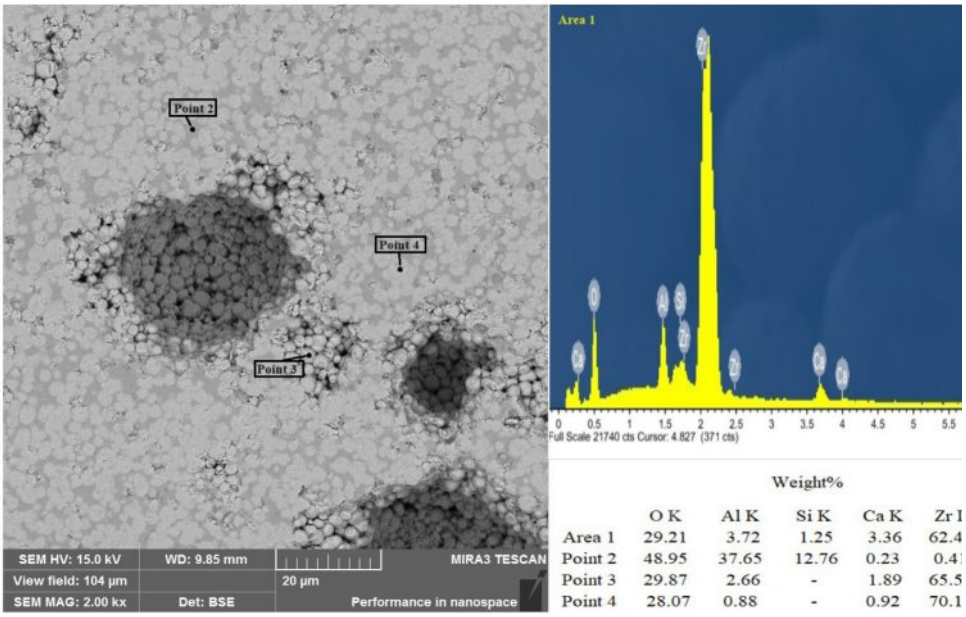


**Fig. 10.** Image of SEM - EDS for 16005CaZ10M.

the increase in cubic phase in the structure despite grain coarsening. The lowest hardness values were obtained in 10% by weight mullite-added CaZ10M samples and the highest hardness were obtained in mullite-free CaZ0M samples.

Considering the microstructural defects observed at high mullite content and sintering conditions, the following aspects will be important to ensure the long-term stability and performance of these composites in practical applications, especially in terms of preservation of mechanical properties over long periods of time:

First of all, some optimization studies can be carried out to minimize the defects caused by high mullite content. On the other hand, mechanical properties such as wear, bending strength, and hardness, as well as water absorption and porosity values should be taken into consideration in this regard. In places where samples with low wear resistance and bending strength will be used, it should be ensured that they are not exposed to high loads and variable loading strains as much as possible. Again, care should be taken not to expose samples with high hardness but low bending strength to high loads. Since the use of samples with relatively high water absorption values due to porosity in humid and aqueous environments may affect the microstructure and therefore the mechanical properties, this issue should also be taken into consideration in zirconia ceramics [34-36].

Another important issue is that if such ceramic composites are exposed to high temperatures for a long time, the stability of the phases in the microstructure and therefore the mechanical properties may be affected. Again, the aging effect, which can occur at low or high temperatures and depends on parameters such as grain size, density, stabilizer, phase diversity in the microstructure, surface quality, processing methods, and processes, should also be taken into consideration as an important issue [37-41]. Therefore, it is important to take these issues into consideration and to control and monitor them.

In order to achieve a better balance between high hardness, flexural strength, and improved wear resistance, additional optimization studies can be carried out by considering the composition and processing parameters below:

The properties of these materials change depending on many parameters such as the sintering temperature and time used in the production process of zirconia ceramic materials, the oxides used for the stabilization of zirconia and their additive ratios, additional additives used to improve microstructure and mechanical properties, production and shaping methods. Therefore, there are many parameters and variables that can be studied for the microstructure and mechanical property optimizations of these ceramics. If an evaluation is needed, especially for the stabilization and additional additive materials we used in our study, some studies can be conducted to reduce microstructural defects by optimizing the sintering temperature and time parameters or by optimizing the composition ratios to obtain a more uniform mullite distribution in the microstructure. It is thought that better results can be obtained and optimized if the mullite contribution rates to the composition are close to 5%, the sintering temperature is close to 1550 ºC, the sintering time is close to values between 1-3 hours and if these values are worked with narrower intervals.

In terms of production and shaping methods, better results can be obtained by using some alternative methods

such as sol-gel, spark plasma sintering, slip and gel casting, hot pressing and hot isostatic pressing. However, these methods also bring some disadvantages such as more complex production processes, high processing costs and more careful control processes.

On the other hand, instead of mullite or together with mullite, some oxides such as yttrium oxide, magnesium oxide, alumina, silicon dioxide, titanium dioxide, lanthanum oxide, boron oxide, phosphorus pentoxide or some compounds such as silicon carbide, silicon nitride, boron nitride, aluminium titanate can be preferred as alternative additives.

## Conclusion and Summary

In this study, Mullite-Calcium Oxide-Zirconium Dioxide composites were produced with various parameters: three sintering temperatures, three sintering times, and three mullite amounts. Some physical tests, hardness, three-point bending strength, characterization studies, and wear resistance of these composites were investigated and compared each other. Drawing from the conducted test and studies, the following inferences have been derived.

With escalating sintering temperature and duration, bulk and relative density, shrinkage, hardness and wear resistance of CaZ0M coded mullite-free samples increased; porosity and water absorption values decreased. However, the low wear resistance values seen in 1600 coded samples despite their high hardness are due to their brittleness as a result of phase variability in the microstructure.

Mullite, cubic zirconia, tetragonal zirconia, and monoclinic zirconia phases were detected in the sample structures.

When all composites with and without mullite additives are evaluated within themselves, as sintering temperature and duration rise, it is observed that the 3-point bending strength values decrease in all samples. With escalating sintering temperature and duration, cubic zirconia phase increases significantly and the hardness increases with it. However, while the amount of cubic zirconia phase in the structure increases, tetragonal zirconia phase decreases and as a result, tetragonal zirconia to monoclinic zirconia transformation toughness decreases, thus the bending strength takes the lowest values.

For 5% (CaZ5M) and 10% (CaZ10M) mullite-added samples with extremely high sintering temperatures and times, decreases in shrinkage, bulk and relative density values are observed due to the defects in the microstructure such as excessive grain growth, large pores, and phase changes. Likewise, due to these reasons, the values decrease as the mullite additive increases in mullite-added samples, which generally have low hardness values.

15001CaZ5M sample has the highest bending strength value and 16005CaZ5M sample has the lowest value. Three-point bending strengths for the mullite-added specimens are generally higher than the mullite-free specimens. This proves that the mullite additive improved the fracture toughness and therefore the bending strength in these samples.

Overall, mullite has been proven to improve wear resistance for these composites. It can be said that CaZ5M (5% mullite-added) composites have the best wear resistance properties.

## Acknowledgements

Authors would like to acknowledge Scientific Research Project Fund of Sivas Cumhuriyet University.

## References

1. T. Kosmač, C. Oblak, P. Jevnikar, N. Funduk, and L. Marion, Dent. Mater. 15[6] (1999) 426-433.
2. T.K. Gupta, J.H. Bechtold, R.C. Kuznicki, L.H. Cadoff, and B.R. Rossing, J. Mater. Sci. 12[12] (1977) 2421-2426.
3. C.B. Abi, O.F. Emrullahoglu, and G. Said, J. Mech. Behav. Biomed. Mater. 18 (2013) 123-131.
4. S. Bhaduri and S.B. Bhaduri, Nanostruct. Mater. 8[6] (1997) 755-763.
5. G.T. Dahl, S. Döring, T. Krekeler, R. Janssen, M. Ritter, H. Weller, and T. Vossmeyer, Materials. 12[18] (2019) 2856.
6. C. Chen, Q. Shen, J. Li, and L. Zhang, J. Wuhan Univ. Technol., Mater. Sci. Ed. 24[2] (2009) 304-307.
7. S.C. Sharma, N.M. Gokhale, R. Dayal, and R. Lal, Bull. Mater. Sci. 25[1] (2002) 15-20.
8. K. Tsukuma and M. Shimada, J. Mater. Sci. 20[4] (1985) 1178-1184.
9. D. Chandra, G. Das, and S. Maitra, Int. J. Appl. Ceram. Technol. 12[4] (2015) 771-782.
10. D.H. Aguilar, L.C. Torres-Gonzalez, L.M. Torres-Martinez, T. Lope, and P. Quintana, J. Solid State Chem. 158[2] (2001) 349-357.
11. S. Vasanthavel, P. Nandha Kumar, and S. Kannan, J. Am. Ceram. Soc. 97[2] (2014) 635-642.
12. V.C. Pandolfelli, J.A. Rodrigues, and R. Stevens, J. Mater. Sci. 26[19] (1991) 5327-5334.
13. C.L. Lin, D. Gan, and P. Shen, J. Am. Ceram. Soc. 71[8] (1988) 624-629.
14. H.L. Chu, C.L. Wang, H.E. Lee, Y.Y. Sie, R.S. Chen, W.S. Hwang, and H.H. Huang, Adv. Mater. Res. 749 (2013) 44-48.
15. B. Stawarczyk, M. Özcan, L. Hallmann, A. Ender, A. Mehl, and C.H. Hämmerlet, Clinical Oral Investigations 17[1] (2013) 269-274.
16. R.K. Govila, J. Mater. Sci. 30[10] (1995) 2656-2667.
17. P.F. Liu, Z. Li, P. Xiao, H. Luo, and T.H. Jiang, Ceram. Int. 44[2] (2018) 1394-1403.
18. A. Duszová, J. Dusza, K. Tomášek, G. Blugan, and J. Kuebler, J. Eur. Ceram. Soc. 28[5] (2008) 1023-1027.
19. V.S. Stubican and S.P. Ray, J. Am. Ceram. Soc. 60 (1977) 534-537.
20. T. Boyraz and A. Akkus, J. Ceram. Proc. Res. 22[2] (2021) 226-231.
21. Y. Wang, A. Zhang, G.D. Li, S.P. Liu, Y. Xiang, and H.F. Cheng, Appl. Compos. Mater. 28 (2021) 321-339.
22. I. Kucuk, T. Boyraz, H. Gökçe, and M.L. Öveçoğlu,

Ceram. Int. 44[7] (2018) 8277-8282.
23. I. Kucuk and T. Boyraz, J. Ceram. Proc. Res. 20[1] (2019) 73-79.
24. Y.Q. Huang, Z. Li, P.F. Liu, T.X. Huang, Y. Li, and P. Xiao, Appl. Surf. Sci. 476 (2019) 232-241.
25. Y. Zhang, W. Jiang, C. Wang, F. Namavar, P.D. Edmondson, Z. Zhu, and W.J. Weber, Phys. Rev. B Condens. Matter Mater. Phys. 82[18] (2010) 184105.
26. S. Nath, N. Sinha, and B. Basu, Ceram. Int. 34[6] (2008) 1509-1520.
27. R.A. Cutler, J.R. Reynolds, and A. Jones, J. Am. Ceram. Soc. 75[8] (1992) 2173-2183.
28. D. Michel, L. Mazerolles, and M. Perez y Jorba, J. Mater. Sci. 18 (1983) 2618-2628.
29. R.H. Hannink, P.M. Kelly, and B.C. Muddle, J. Am. Ceram. Soc. 83[3] (2000) 461-487.
30. P. Ganeshan, Y. Sravani, K. Raja, and B.K. Singh, J. Ceram. Proc. Res. 24[5] (2023) 781-787.
31. G. Gokilakrishnan, B.K. Singh, and M. Vigneshkumar, J. Ceram. Proc. Res. 24[4] (2023) 655-661.
32. Y. Zhang, Dent. Mater. 30[10] (2014) 1195-1203.
33. Y.Q. Huang, P.F. Liu, Z. Li, and P. Xiao, Ceram. Int. 44[17] (2018) 21882-21892.
34. M. Yoshimura, T. Noma, K. Kawabata, and S. Somiya, J. Mater. Sci. Lett. 6 (1987) 465-467.
35. T. Sato, S. Ohtaki, T. Endo, and M. Shimada, Adv. Ceram. (Westerville, OH, U. S.) 24 (1988) 501-508.
36. S. Lawson, J. Eur. Ceram. Soc. 15[6] (1995) 485-502.
37. M. Dehestani and E. Adolfsson, Int. J. Appl. Ceram. Technol. 10[1] (2013) 129-141.
38. J. Munoz-Saldana, H. Balmori-Ramirez, D. Jaramillo-Vigueras, T. Iga, and G.A. Schneider, J. Mater. Res. 18 (2003) 2415-2426.
39. J. Chevalier, S. Deville, E. Munch, R. Jullian, and F. Lair, Biomaterials 25 (2004) 5539-5545.
40. J.D. Lin, J.G. Duh, and C.L. Lo, Mater. Chem. Phys. 77 (2002) 808-818.
41. H.B. Lima, K.S. Oha, Y.K. Kima, and D.Y. Lee, J. Mater. Sci. Eng. A 483 (2008) 297-301.